Talanta 145 (2015) 43–54

Contents lists available at ScienceDirect

Talanta

journal homepage: www.elsevier.com/locate/talanta

Low-cost bioanalysis on paper-based and its hybrid microfluidic platforms

Maowei Dou [a], Sharma Timilsina Sanjay [a], Merwan Benhabib [b], Feng Xu [c,d], XiuJun Li [a,e,f,*]

[a] Department of Chemistry, University of Texas at El Paso, 500 West University Ave, El Paso, TX 79968, USA
[b] OndaVia Inc, Hayward, CA 94545, USA
[c] The MOE Key Laboratory of Biomedical Information Engineering, School of Life Science and Technology, Xi'an Jiaotong University, Xi'an 710049, PR China
[d] Bioinspired Engineering and Biomechanics Center, Xi' an Jiaotong University, Xi' an 710049, PR China
[e] Department of Biomedical Engineering, University of Texas at El Paso, 500 West University Ave, El Paso, TX 79968, USA
[f] Border Biomedical Research Center, University of Texas at El Paso, 500 West University Ave, El Paso, TX 79968, USA

ARTICLE INFO

Article history:
Received 24 February 2015
Received in revised form
20 April 2015
Accepted 22 April 2015
Available online 6 May 2015

Keywords:
Low-cost bioassays
Paper-based microfluidic lab-on-a-chip
Paper hybrid microfluidic platform
Disease diagnosis
Food safety analysis

ABSTRACT

Low-cost assays have broad applications ranging from human health diagnostics and food safety inspection to environmental analysis. Hence, low-cost assays are especially attractive for rural areas and developing countries, where financial resources are limited. Recently, paper-based microfluidic devices have emerged as a low-cost platform which greatly accelerates the point of care (POC) analysis in low-resource settings. This paper reviews recent advances of low-cost bioanalysis on paper-based microfluidic platforms, including fully paper-based and paper hybrid microfluidic platforms. In this review paper, we first summarized the fabrication techniques of fully paper-based microfluidic platforms, followed with their applications in human health diagnostics and food safety analysis. Then we highlighted paper hybrid microfluidic platforms and their applications, because hybrid platforms could draw benefits from multiple device substrates. Finally, we discussed the current limitations and perspective trends of paper-based microfluidic platforms for low-cost assays.

1. Introduction

The microfluidic lab-on-a-chip (LOC), a miniaturized device mostly produced by the microfabrication technique, has developed rapidly in the last few decades [1], since its advent in the 1990s. Microfluidic devices have been widely used in various applications, especially in bio-applications, thanks to their significant advantages (e.g. fast analysis, low reagent consumption, and high capillary electrophoresis separation efficiency) associated with their inherent miniaturization, integration, portability and automation [1–10]. Various modern instruments (e.g. real-time polymerase chain reaction, or qPCR [11,12]) have been developed for biological assays and environment monitoring. However, many of such instruments are expensive and bulky, which limits their use in resource-poor settings. Miniaturized devices with high portability have great potential for point of care (POC) applications beyond laboratory settings, such as disease diagnosis [13–16], food safety inspection [17,18], and environmental analysis [19–21]. Various materials including silicon [22], glass [23–28], polymer (e.g. polydimethylsiloxane (PDMS), poly (methyl methacrylate) (PMMA)) [29–31], and paper [32–36] have been used for microfluidic platform fabrication. However, the different properties of these materials resulted in different fabrication approaches and applications of their corresponding devices. For example, due to high material cost, lack of rapid prototyping, stringent requirements on cleanroom facility, low biocompatibility and difficulty of optical detection, silicon-based microfluidic platforms are not well suited to POC applications for low-resource settings, such as developing nations.

Paper is an inexpensive and abundant cellulose fiber web with three-dimensional (3D) microstructures and a high surface-to-volume ratio property. The biodegradable cellulose paper can transport fluids via the capillary effect without the need of external pneumatic pumps or electric power, making paper an ideal substrate for a disposable equipment-free testing solution. Paper has been used for analytical and clinical chemistry since the early 20th century [1]. The low-cost, easy-to-use paper-based testing strips for testing pH, pregnancy and diabetes have been commercially available for decades. Since the Whitesides group introduced integrated paper-based microfluidic devices [37] to

* Corresponding author at: Department of Chemistry, University of Texas at El Paso, 500 West University Ave, El Paso, TX, 79968, USA. Tel.: +1 915 74 8967; fax: +1 915 747 5748.
E-mail address: xli4@utep.edu (X. Li).

http://dx.doi.org/10.1016/j.talanta.2015.04.068
0039-9140/

offer low-cost and easy-to-use LOC platforms, paper has become one of the most prevalent substrates for low-cost bioassays [34,35,38,39], such as immunochromatographic strips (ICS) for quantitative or semi-quantitative assays [40].

Different materials have their own advantages and limitations. Despite its significant advantages, paper also has its own limitations. For instance, generally paper is not transparent, though there are efforts to develop optically transparent paper [41,42]. Paper substrates lack the high performance in flow control demonstrated by polymer substrates. Therefore, paper hybrid microfluidic platforms have been developed which can draw benefits from multiple device substrates [14,15]. These hybrid platforms include paper/PDMS hybrid systems [14,15,36], paper/cotton thread hybrid systems [43,44] and others [45].

This review paper mainly focuses on recent advances of low-cost bioanalysis using paper-based microfluidic platforms, more specifically fully paper-based and paper hybrid microfluidic platforms, especially in resource-poor settings. We will first summarize the fabrication techniques and the applications of fully paper-based microfluidic platforms, with an emphasis on applications in human health diagnostics (via proteins, nucleic acids and cellular analysis) and food safety analysis. Then we will highlight paper hybrid microfluidic platforms for various low-cost bioassays. Finally, we will discuss the current limitations and prospective trends of paper-based microfluidic platforms.

2. Fully paper-based microfluidic platforms

2.1. Fabrication techniques for paper-based microfluidic platforms

Different types of paper are suitable as building materials for paper-based microfluidic platforms, e.g. cellulose paper, nitrocellulose paper/membrane. The selection of the appropriate type relies on the technologies of fabrication and the field of its applications. Cellulose paper is widely used by most researchers because of its affordability, naturally hydrophilic properties and fast liquid penetration. Whatman filter paper is the most popular among the various types of cellulose paper [20,46–48], with well categorized porosity, flow rate and particle retention. For example, as standard grade filter paper, Whatman filter No. 1 (pore size 11 μm) allows medium flow rates and particle retention, which is widely adopted since it is compatible with many patterning techniques [20,46,47,49–55]. Whatman No. 4 filter paper has larger pore size (20–25 μm), which is ideal for the fabrication technique of etch printing that requires a solvent to swell the cellulose fibers and restrict the pore size [48]. Due to the high porosity of paper, electrodes can be manually screen printed on paper for electrochemical detection [19,56]. Chemically modified cellulose paper blended with an inorganic filler (e.g., polyester) is commercially available as an ion-exchange substrate. It is non-degradable and presents a smoother surface, which is suited to surface chemical modification [19,57]. The hydrophobic nitrocellulose membrane is another important type of paper substrate. With a smooth surface and uniform pore size (0.45 μm), it allows for a more reproducible and stable liquid flow. This type of paper has a high degree of non-specific binding property towards biomolecules, which makes it suitable for immobilization of DNA [58], proteins [47,50,59–62] and cells [63].

Paper-based microfluidic platforms rely on the capillary action to circulate fluids. When patterned with microstructures, paper becomes a platform in which sample preparation, purification and multiple bioreactions can occur simultaneously without cross-contamination. There are three major patterning principles of microstructures on paper-based microfluidic platforms: physical blocking of pores in paper, physical deposition of reagents on the fiber surface, and chemical modification of the paper surface. Photolithography [50] and plotting [64] are the principal techniques of physical blocking of pores in paper, in which paper is treated with chemicals of photoresist (e.g., SU-8) and PDMS to define patterns. Techniques of physical deposition of reagents on fiber surfaces include inkjet etching [65], wax printing [62,66], screen printing [67], and flexography printing [68], among others. Plasma treatment [69] and inkjet printing [48] are the main techniques for chemical modification of the paper surface. In the following sections we focus primarily on photolithography and wax printing.

2.1.1. Physical blocking of pores in paper

The technique of photolithography for patterning a paper-based microfluidic device requires a copier machine or an inkjet printer, UV light and a hot plate. The fabrication procedures which take less than 30 min are described in Fig. 1 [50]. First, a transparent film is prepared, on which the microfluidic pattern is printed. Then a sheet of paper is impregnated with a photoresist (e.g., SU-8) and subsequently incubated. After incubation, the front side of the treated paper is covered with a transparent film (i.e., a photomask) from the last step, and the backside is covered with a sheet of black backing paper to avoid light reflection. After UV light exposure, the paper sheet is baked, and the excessive photoresist is removed with a mixture of acetone and isopropyl alcohol. Photolithography is capable of creating features down to 100 μm in size and hydrophobic barriers as small as 200 μm in width. The major material cost in the photolithography patterning technique is the photoresist. For example, SU-8 and PMMA cost $1/g and $0.15/g respectively [64]. This technique requires organic solvents, which may damage the flexibility of the paper, making the fabricated paper devices susceptible of folding and bending [54,67,70].

Compared to the multi-step photolithographic process, plotting is a more direct way to define hydrophobic patterns on paper by printing the hydrophobic polymer. As an inexpensive, non-toxic, and readily available polymer, PDMS is commonly used in the plotting fabrication technique. Bruzewicz et al. [64] first investigated this technique when modifying a plotter to print a hexane solution of PDMS onto filter paper as hydrophobic barriers. This method does not damage the flexibility of the paper, but it has

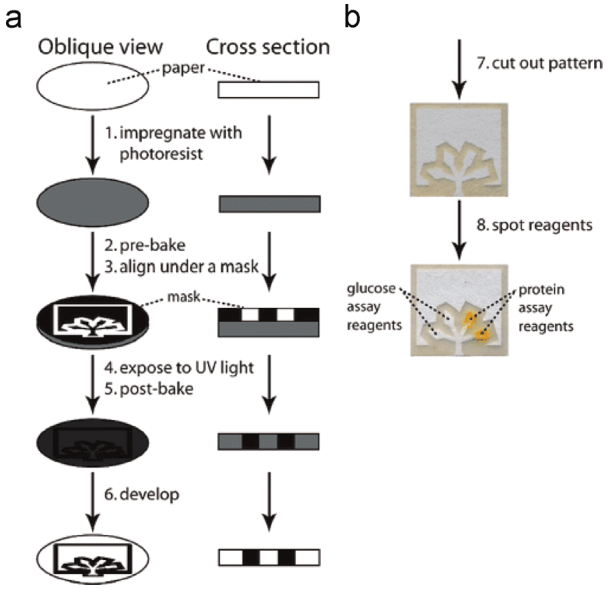

Fig. 1. Schematic of the photolithography technique for fabricating paper-based microfluidic platforms: (a) procedure for patterning paper with hydrophobic photoresist, (b) derivatization of the device for bioassays (*Source*: Adapted with permission from Martinez et al., 2008. Copyright © 2008 American Chemical Society [50]).

other limitations. For example, since paper is a non-uniform porous substrate, it does not permit a controllable penetration of PDMS [69]. Herein, although the smallest feature and barrier were reported to be 1 mm, in practice, 2–4 mm wide channels are needed since patterned lines are hardly straight. In addition, it is time consuming, which takes 1 h at 70 °C for PDMS to cure [64].

2.1.2. Physical deposition of reagents on paper surface

Compared to the multi-step photolithography, wax printing is simpler, less expensive, more flexible for changes in the device design, and adapted to mass manufacturing. Wax is another hydrophobic plastic material that was proposed by the Whitesides group and the Lin group for fluidic barriers on paper [62,66]. Wax is inexpensive, easy to obtain, non-toxic, biodegradable, insoluble in water and malleable at ambient temperature. This technique is rapid (~5 min) and does not require any solvents, relying on only two pieces of equipment – a commercially available solid-ink printer and a hot plate or oven. In wax printing, a pattern of wax is first deposited on a sheet of paper using a solid-ink printer. Then the paper is heated to melt the wax and diffuse it throughout the entire thickness of the paper. Wax has the advantage of avoiding the use of organic solvents. The disadvantage of this method is that the melted wax in paper spreads in all directions by capillarity, which renders the patterns ill-defined and lacking in high resolution. However, for a given heating time at a certain temperature, the spreading distance is constant. For example, a spreading distance of 300 μm was measured when heating at 150 °C for 120 s, resulting in barrier and channel widths of 850 μm and 560 μm, respectively [66]. Several solutions have been presented to improve the resolution. For example, by the use of nitrocellulose paper which has more uniform and smaller pores, more controlled and precise wax patterns were reported with channels as thin as 300 μm and barriers of 60 μm [61]. In addition, vacuum can be applied to minimize lateral spreading. Wax is insoluble in water but soluble in nonpolar organic solvents, which can make wax-printed devices erode in organic solvents. Additionally, the colorants in the wax layers can be leached out by highly corrosive solvents, such as alcohols, acetone and chloroform.

Compared to wax printing, screen printing is simpler and adequate for developing countries where wax-printers are expensive and not readily available [67]. Screen printing requires a mesh. Solid wax can be transferred through the mesh when it is pressed. Controlled by the size of the mesh, wax is loaded and fully blocks the coating areas on a sheet of paper. Then, similarly to wax printing, the wax on the paper is heated to melt to form a hydrophobic barrier throughout the entire thickness of the paper. The penetration of the wax can be controlled by adjusting the heating temperature and time. A linear relationship has been found between the width of the deposited hydrophobic barrier and the width of the design on the mask. The minimum channel and barrier widths that can be achieved by screen printing were 0.65 mm and 1.3 mm respectively [67], whereas the minimum feature size from wax printing is 300 μm, indicating higher resolution of wax printing than screen printing.

Inkjet etching is also a simple method to pattern hydrophobic barriers using a printer. It comprises two steps: filter paper is first soaked in a 1.0 wt% solution of polystyrene in toluene for 2 h to become completely hydrophobic; then the modified paper is dried at room temperature for 15 min, and patterned by inkjet printing of toluene, which is to dissolve the polymer and precisely re-expose hydrophilic areas for fluidic paths [65]. For example, a 550 μm wide flow channel was printed on the filter paper by inkjet etching with a sensing area of 1.5 mm × 1.5 mm for simultaneous measurement of pH, total glucose and protein [65]. This technique is time consuming (~2 h) with multiple printing runs. In addition, it requires a customized potentially expensive inkjet printer [67].

Flexographic printing is a technique that patterns polystyrene boundaries onto chromatographic paper [68]. Polystyrene is one of the most popular hydrophobizing agents used in this technique since it is biocompatible and does not require heat treatment. Patterns of polystyrene are formed on the front side of a sheet of paper with 5% polystyrene ink, which partially penetrates the paper thickness. A uniform polystyrene layer is printed on the backside to waterproof the entire paper thickness. This flexographic printing technique is compatible with roll-to-roll mass production by using existing tools available in printing houses. Channels of 500 μm in width with boundary roughness of 30 μm were reported, with negligible lateral ink spreading [68].

2.1.3. Chemical modification

Chemical modification of the paper surface is a simpler and more affordable approach than pore filling or deposition. Alkyl ketene dimer (AKD) and alkenyl succinic acid anhydrate (ASA) are low-cost patterning reagents that are commonly used for changing the wetting properties of the cellulose pulp and imparting hydrophobicity by esterification of the hydroxy group of the cellulose [70]. As an important advantage of this approach, the treated paper can retain its original flexibility and bendability, making packaging and handling easier. Additionally, there are no visible marks or changes of color on the hydrophobic areas of paper devices, which is critical for colorimetric-based bioassays.

Inkjet printing that uses a digital inkjet printer can accurately deposit an AKD–heptan solution to create hydrophobic barriers on paper [48]. Paper devices are first heated after printing for curing. Then, bio-indicators in the sensing zones are deposited by using the same printer. As a low-cost, easy and rapid fabrication process, inkjet printing can be adapted to mass manufacturing. This process provides paper devices with fine fluidic channels together with preserved folding and bending capability [71]. In addition, being a non-contact liquid deposition, it effectively minimizes cross-sample contamination and decreases risk of substrate damage, which is highly desirable for the printing of biomolecules [70,72,73].

2.1.4. Other techniques

Laser printing is a one-step patterning method that uses a CO_2 laser to pattern hydrophilic areas on a hydrophobic paper substrate, such as parchment, wax or palette paper [74]. Oxidized hydrophilic groups are formed on the treated substrate surface, which can trap chemicals but not allow lateral diffusion of liquid. High speed and high resolution (62 μm) can be achieved by using this technique.

Paper cutting and taping is the simplest method to fabricate paper-based devices. Cutting is rapid and only requires a pair of scissors, or computer-controlled cutting equipment such as a laser cutter for more complex patterns [14,15,56]. Tape is necessary to support any free-standing structures. By using a computer controlled knife on an XY plotter, Fenton et al. fabricated a nitrocellulose lateral flow device shaped in two dimensions [47]. Afterward, the cut paper device was sandwiched between a vinyl and a polyester film, minimizing dehydration, evaporation and preventing external contaminations. Cutting is suitable for mass manufacturing and compatible with any type of cellulosic substrates. The smallest feasible dimensions for an arm and a hole are 1 mm and 0.7 mm diameter, respectively. However, the cutting tool is expensive (~$5,000). In addition, fabrication of 3D paper-based devices has been demonstrated using double-sided adhesive [75].

2.2. Applications of paper-based microfluidic platforms

2.2.1. Human health diagnostics

Physiological signals that reflect the biological state changes of an unhealthy person can be evaluated by testing disease biomarkers or molecular indicators of normal, pathogenic, treatment or recovery

processes. These biomarkers include nucleic acids (DNA or RNA), proteins, lipids, or metabolite biomarkers, are highly specific, and thus can be used to diagnose various diseases accurately [76–78]. For example, prostate specific antigen (PSA) has been widely used to screen and monitor prostate cancer [79]. The best biomarkers should be accurate, as non-invasive as possible, and easy to use for testing. Tissue, urine and serum samples have been widely used as the source of biomarkers. In addition, the diagnostic platforms for these biomarkers should be affordable, sensitive, user-friendly, and mass producible for POC analysis according to the World Health Organization (WHO). Paper-based microfluidic platforms, as mentioned before, are a strong low-cost contender for this kind of diagnosis. Recent advances in paper-based bioassays for human health diagnostics can be separated into the following three categories: proteins, nucleic acids and cells, based on different categories of analytes, as summarized in Table 1. Table 1 also shows that cancer biomarker detection attracts great interest.

2.2.1.1. Proteins analysis. Proteins are one kind of the most widely used biomarkers for disease diagnostics. Protein analysis that often uses immunoassay techniques includes enzyme linked immunosorbent assay (ELISA) [80], immunofluorescence [81], western blotting [82] and immunodiffusion [83]. Traditionally, most of these detection methods are complicated and require expensive instruments. For example, ELISA is one of the most commonly used techniques. However, it takes hours to complete (or even overnight) and relies on expensive instruments (e.g. microplate readers) [84,85]. Therefore, there is a great need to develop low-cost, simple and rapid POC diagnostic approaches with high sensitivity, especially for resource-limited settings. Recently, a number of paper-based microfluidic platforms were reported for the analysis of protein biomarkers of cancers and infectious diseases using colorimetric, fluorescence, electrochemical and electrochemiluminescence (ECL) detection methods.

Colorimetric immunoassay, one of the most widely used detection methods, is based on the color change due to chemical reaction

Table 1
Summary of human health diagnostics on paper-based & its hybrid microfluidic platforms.

Category	Analyte	LOD	Application	Microfluidic platform	Fabrication method	Reference
Proteins analysis	BSA	0.38 μM	–	Paper	Photolithography	[37]
	BSA	3.672 μM	–	Paper/cotton	–	[44]
	rabbit IgG	54 fmol/zone	–	Paper	Photolithography	[60]
	rabbit IgG	3.9 fM	–	Paper	Photolithography	[33]
	goat IgG	20 ng/mL	–	Paper	Paper cutting	[89]
	mouse IgG	0.33 ng/mL	–	Paper	–	[91]
	HIV-1 envelope antigen gp41	–	HIV diagnosis	Paper	Photolithography	[60]
	AFP	0.06 ng/mL	Cancer diagnosis	Paper	Wax-screen-printing	[87]
	AFP	0.15 ng/mL	Cancer diagnosis	Paper	Wax printing, screen printing	[13]
	CA-125	0.33 U/mL	Cancer diagnosis	Paper	Wax-screen-printing	[87]
	CA-125	0.6 U/mL	Cancer diagnosis	Paper	Wax printing, screen printing	[13]
	CA-125	0.2 mU/mL	Cancer diagnosis	Paper	Wax printing, screen printing	[56]
	CEA	0.05 ng/mL	Cancer diagnosis	Paper	Wax-screen-printing	[87]
	CEA	0.8 pg/mL	Cancer diagnosis	Paper	Wax printing	[88]
	CEA	0.5 ng/mL	Cancer diagnosis	Paper	Wax printing, screen printing	[13]
	CEA	0.01 ng/mL	Cancer diagnosis	Paper	Wax printing, screen printing	[56]
	PSA	1.0 pg/mL	Cancer diagnosis	Paper	Wax printing	[88]
	CA19-9	0.17 U/mL	Cancer diagnosis	Paper	Wax printing, screen printing	[13]
Nucleic acids analysis	dengue virus serotype-2 RNA	300 ng/mL	Dengue fever detection	Paper	Wax printing	[95]
	N. meningitidis DNA	3 copies/zone	Bacterial meningitis detection	Paper/PDMS	–	[15]
	CYP2C19 gene	–	Genetic testing	Paper/glass microcapillary	–	[45]
Cellular analysis	MCF-7	250 cells/mL	Cancer diagnosis	Paper	Wax printing	[99]
	HL-60	350 cells/mL	Cancer diagnosis and treatment	Paper	Wax printing	[100]
	K562	400 cells/mL	Cancer diagnosis and treatment	Paper	Wax printing	[101]
	P. aeruginosa	500 cfu/ml	Cystic fibrosis diagnosis	Paper	–	[105]
	S. aureus	500 cfu/ml	Cystic fibrosis diagnosis	Paper	–	[105]
	S. typhi	1.14×10^5 cfu/mL	Typhoid fever diagnosis	Paper	–	[106]
Others	glucose	0.25 mM	Human health diagnosis	Paper	Photolithography	[37]
	NO_2^-	–	Human health diagnosis	Paper/thread	–	[43]
	NO_2^-	0.147 mM	Human health diagnosis	Paper/cotton	–	[44]
	UA	–	Human health diagnosis	Paper/thread	–	[43]
	UA	125.625 μM	Human health diagnosis	Paper/cotton	–	[44]
	urobilinogen	4.861 μM	Human health diagnosis	Paper/cotton	–	[44]

between the enzymes linked to the analytes and the colorimetric reagents. Many researchers have made striking advances in the field. For instance, Martinez et al. [37] demonstrated a simple paper-based microfluidic device for the simultaneous detection of glucose and a protein bovine serum albumin (BSA) in 5 μL of urine. The glucose assay was based on the enzymatic oxidation of iodide to iodine, resulting in a color change from clear to brown. The protein assay was based on the color change of tetrabromophenol blue (TBPB). When it was ionized and bound to the protein, the color changed from yellow to blue. Artificial samples of glucose and protein in clinically relevant ranges (2.5–50 mM for glucose and 0.38–7.5 μM for bovine serum albumin) were measured. Cheng et al. [60] described colorimetric ELISA performed in a 96-microzone paper-based device (P-ELISA). This paper-based device included an array (12×8) of circular test zones (the same layout and dimensions as a standard plastic 96-well plate) for running multiple P-ELISAs in parallel. ELISA was performed using alkaline phosphatase as the enzyme and BCIP/NBT (5-bromo-4-chloro-3-indolyl phosphate and nitro blue tetrazolium) as the substrate. The limit of detection (LOD) of rabbit IgG using the P-ELISA was found to be 54 fmol/zone. They also demonstrated the detection of HIV-1 envelope antigen gp41 in a spiked human serum sample. The positive result was distinguishable even after a ten-fold dilution of the human serum. Songjaroen et al. [86] developed a paper-based microfluidic device to separate blood plasma from whole blood and to quantify plasma protein in a single step, which was significant for the consequent diagnostics. The device consisted of of blood separation membrane combined with patterned Whatman No. 1 paper. Without dilution, plasma was effectively separated from a single drop of whole blood (15–22 μL) in a wide range of hematocrit (24–55%) within 2 min. Plasma protein detection using bromocresol green (BCG) colorimetric assay showed no significant difference from conventional methods ($p > 0.05$, pair t-test).

Chemiluminescence relies on measuring the light emitted by certain chemical reactions. Wang et al. [87] reported a paper-based microfluidic device to perform chemiluminescence ELISA. In this platform, capture antibodies were immobilized in paper hydrophilic zones through glutaraldehyde cross-linking. 4-iodophenol-enhanced luminol chemiluminescence assay was performed on the horseradish peroxidase (HRP)-labeled antibodies. Chemiluminescence ELISA was successfully performed with a linear detection range of 0.1–35.0 ng/mL for α-fetoprotein (AFP, a biomarker for hepatocellular carcinoma), 0.5–80.0 U/mL for cancer antigen 125 (CA-125, a biomarker for ovarian cancer) and 0.1–70.0 ng/mL for carcinoembryonic antigen (CEA, a biomarker for colorectal cancer). In addition, this lab-on-paper immunodevice can provide reproducible results upon storage at 4 °C (sealed) for at least 5 weeks.

Electrochemiluminescence (ECL) that combines electrochemical and luminescence techniques can provide good selectivity and sensitivity wherein a set of electrodes is used to trigger and control a chemiluminescence reaction involving a luminophore compound. Li et al. [88] showed a battery-triggered ECL multiplexed immunoassay using a dual-signal amplification strategy on a paper-based microfluidic device. They used a graphene oxide-chitosan/gold nanoparticle (GCA) immunosensing platform and P-acid functionalized nanoporous silver (P-acid/NPS) for signal amplification. They showed that PSA and CEA could be sequentially detected in the linear ranges of 0.003–20 ng/mL and 0.001–10 ng/mL with the LOD down to 1.0 and 0.8 pg/mL, respectively. Ge et al. [13] demonstrated a wax-patterned 3D paper-based ECL microfluidic platform with screen-printed electrodes for the measurement of four tumor biomarkers in real clinical serum samples. As shown in Fig. 2, four different capture antibodies for AFP, CA-125, cancer antigen 19-9 (CA19-9, biomarker for pancreatic cancer), and CEA were immobilized on the eight working electrodes sequentially placed into the circuit to trigger the ECL reaction. The limits of detection at a signal-to-noise ratio of 3 were found to be 0.15 ng/mL, 0.6 U/mL, 0.17 U/mL, and 0.5 ng/m for AFP, CA-125, CA19-9, and CEA, respectively.

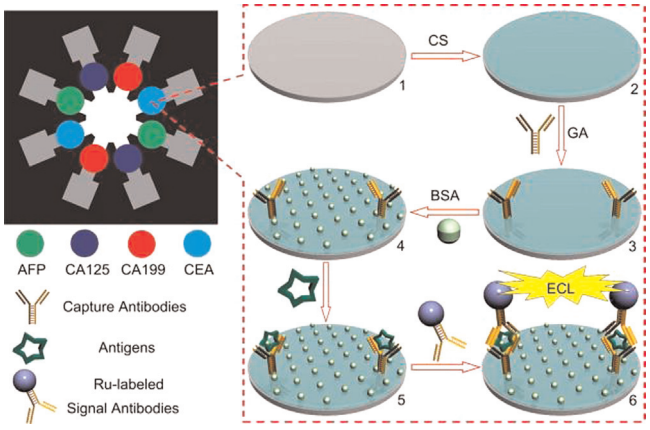

Fig. 2. A 3D paper-based ECL microfluidic platform for multiplexed measurement of four cancer biomarkers: 1) screen-printed carbon working electrode; 2) chitosan (CS) modification; 3) immobilization of capture antibodies; 4) blocking and washing; 5) capturing and washing; 6) incubation with signal antibodies, washing and triggering ECL reaction (*Source*: Adapted with permission from Ge et al., 2012. Copyright © 2012 Elsevier [13]).

Electrochemical detection is another most widely used detection methods in paper-based microfluidic platforms due to the ease of miniaturization and integration of electrodes on a microfluidic device. Li et al. [33] described an electrochemical ELISA on a paper-based microfluidic device, on which working and counter electrodes were screen-printed from graphite ink, and a reference electrode from silver/silver chloride ink. The electrochemical ELISA of IgG was demonstrated with LOD of 3.9 fM achieved. Wang et al. [56] demonstrated the electrochemical immunoassay of CA-125 and CEA on a 3D wax-patterned paper-based microfluidic platform. Antibodies for CA-125 and CEA were immobilized on paper with chitosan and cross-linking with glutaraldehyde, allowing both tumor markers to be simultaneously detected. Simultaneous detection of two tumor markers in real clinical serum samples showed a linear range of 0.001–75.0 U/mL for A-125 and 0.05–50.0 ng/mL for CEA. The limits of detection for CA-125 and CEA were 0.2 mU/mL and 0.01 ng/mL, respectively.

Fluorescence detection on paper-based microfluidic platforms has shown good analytical performance. Liang et al. [89] demonstrated a paper strip fluoroimmunoassay for the detection of IgG. Polystyrene (PS) microbeads conjugated with primary anti-goat IgG were immobilized on paper strips for capturing IgG. Anti-goat IgG-cy3 was used as the secondary antibody for fluorescence detection. The LOD of 20 ng/mL was achieved using a fluorescence array scanner. Yu et al. [90] used divinyl sulfone (DVS) chemistry to immobilize small molecules, proteins and DNA covalently onto hydroxyl group of the cellulosic paper for fluorescence detection. Protein–carbohydrate and protein–glycoprotein interactions as well as oligonucleotide hybridization indicated that the membrane's bioactivity was specific, dose-dependent, and stable over a long period of time. Fluorescence detection demonstrated that DVS-modified cellulose paper was suitable for the conjugation of carbohydrates and the analysis of biological interaction. The LOD of nucleic acid was as low as 500 pM. This kind of DVS chemistry could be used for the conjugation of biomolecules for biomedical applications of human health diagnostics. Although high sensitivities could be obtained by a paper-based fluorescence immunoassay, external instrumentation such as a fluorescence scanner is often required, which limits its application for POC bioassays.

Surface-enhanced resonance Raman scattering (SERRS) has also been employed in paper-based immunoassay. For example, Chen et al. [91] demonstrated a paper-based SERRS immunoassay. They used modified antibodies conjugated to magnetic beads to capture

mouse IgG. Detection was conducted on a silver colloid/PVP/filter paper SERRS substrate. After magnetic separation, 5-bromo-4-chloro-3-indolyl phosphate (BCIP), a low SERRS active compound, was added as the substrate for ALP to generate a high SERRS response, which could detect mouse IgG from 1–500 ng/mL with a LOD of 0.33 ng/mL.

2.2.1.2. Nucleic acids analysis. Nucleic acid analysis has been widely used in many areas, including clinical diagnostics. It can detect the etiologic agents of diseases directly from clinical samples, which is very useful in rapid detection of unculturable or fastidious microorganisms. Additionally, it allows for sensitive identification and characterization of pathogens by using amplified microbial DNA/RNA. Usually, a limited amount of DNA/RNA is available (e.g. only a single copy of specific DNA in a cell), particularly when analyzing biological human samples. Therefore, amplification of the target sequence is a key step in nucleic acid analysis to enhance the assay sensitivity [92]. Nucleic acid biomarkers can be quantified during the amplification step (e.g. by qPCR [93]), or after the amplification step (e.g. through DNA hybridization).

As a low-cost, portable, disposable and fast nucleic acid detection method, microfluidic paper-based nucleic acid hybridization has attracted great interest among researchers. Araújo et al. [94] presented an activated paper-based microfluidic strip bearing cy3-labeled single-stranded probe DNA (ssDNA) for rapid target hybridization via capillary transport. By using the inexpensive and readily available bifunctional linking reagent, 1,4-phenylenediisothiocyanate, a one-step activation of the Whatman No. 1 filter paper was developed, making it amenable to subsequent coupling of cy3-labeled ssDNA. Because of the intrinsic wicking ability of the paper matrix, which facilitated rapid sample elution through arrays of the probe DNA, hybridization was achieved in less than 2 min. The paper-based microfluidic strip for rapid and specific DNA diagnostics was exemplified by the discrimination of amplicons generated from canine and human mitochondrial and genomic DNA in mock forensic samples. Cheng et al. [95] reported a paper-based colorimetric assay for monitoring the dengue virus by examining the amplified products. The results indicated that their paper-based microfluidic device was capable of detecting the amplified products with a concentration of 6×10^5 plaque-forming units (pfu)/mL (300 ng/mL). Cunningham et al. [96] reported an inexpensive paper-based microfluidic device for quantitative detection of nucleic acids, which was based on the principle of target-induced conformational switching of an aptamer linked to an electrochemical label. The LOD for DNA was 30 nM, and good reproducibility was demonstrated. Ihalainen et al. [97] developed two different supramolecular recognition architectures for impedimetric detection of DNA hybridization on paper-based inkjet-printed gold electrodes. The first architecture comprises alternating layers of biotinylated self-assembly monolayer (SAM), streptavidin and the biotinylated DNA probe. The second architecture consists of immobilized thiol-functionalized DNA probe (HS-DNA) and subsequent backfill with 11-mercapto-1-undecanol (MUOH) SAM. According to the electrochemical impedance spectroscopy (EIS) measurement results, it showed that the hybridization could be detected with impedimetric spectroscopy in picomolar range for both systems. Wang et al. [98] reported a paper-based photoelectrochemical (PEC) microfluidic platform for sensitive DNA detection, which used a graphene-modified porous Au-paper electrode as the working electrode to obtain enhanced PEC responses. The quantification mechanism was based on the charging of a novel paper supercapacitor (PS) constructed on the platform by the generated photocurrent. The PS was automatically shorted after a fixed period of time to output an instantaneously amplified current, which was sensitively detected by a terminal digital multi-meter (DMM) integrated with the microfluidic platform. It was demonstrated that this paper-based microfluidic platform could detect DNA at the femtomolar level.

Despite the good performance of the microfluidic paper-based nucleic acid hybridization for nucleic acid detection, DNA hybridization based assays on paper-based devices still rely on a nucleic acid amplification process performed off-chip that often requires support of expensive and bulky equipment in laboratory settings. It is still challenging to integrate DNA amplification steps on a paper-based device, due to issues of liquid evaporation and heating element requirements.

2.2.1.3. Cellular analysis. Various cyto-sensors based on chemiluminescent, fluorescent, electrochemical, electrochemiluminescence and colorimetric detection have been developed for detection of cancer cells and other types of mammalian cells with high selectivity and sensitivity. The development of low-cost and easy-to-use microfluidic paper-based cyto-devices offers an encouraging potential for miniaturized and high-throughput detection of cancer cells or bacteria, separation of blood cells and 3D cell culture.

Various paper-based cyto-sensors have been developed for cancer research. Wu et al. [99] developed a microfluidic paper-based electrochemiluminescence origami cyto-device (μ-PECLOC) for the specific capture of cancer cells, indicating the potential applications of multiple early cancer diagnosis and clinical treatment. Aptamers-modified Au/paper electrodes were employed in the μ-PECLOC as working electrodes. Due to the specific recognition of mannose on cell surface, concanavalin-A conjugated porous Au/Pd alloy nanoparticles were introduced into the μ-PECLOC as catalytically promoted nanolabels for peroxydisulfate ECL detection. The μ-PECLOC demonstrated good analytical performance towards the cyto-sensing of four types of cancer cells (Human breast adenocarcinoma cells (MCF-7), human acute promyelocytic leukemia cells (HL-60), human chronic myelogenous leukemia cells (K562), and human acute lymphoblastic leukemia cells (CCRF-CEM)) with good stability, reproducibility and accuracy. The linearity for MCF-7 cells was in the range of 450–1.0×10^7 cells/mL with the LOD of 250 cells/mL. The reproducibility was investigated based on inter-assay precision between 10 μ-PECLOCs. The relative standard deviations for the parallel detection of 500, 10^4, and 10^7 MCF-7 cells/mL were 3.64%, 3.33%, and 3.76%, respectively. Su et al. [100] developed a microfluidic paper-based electrochemical cyto-device (μ-PECD) for detection of cancer cells and in situ screening of anticancer drugs in a multiplex manner based on in-electrode 3D cell culture. This entire μ-PECD was fabricated on a single sheet of flat paper in batches based on the principle of kirigami and origami, with aptamer-modified Au/paper electrodes integrated on the chip. This μ-PECD, could respond down to four human acute promyelocytic leukemia cells (HL-60) in 10 μL volume with a wide linear calibration range from 5.0×10^2 to 7.5×10^7 cells/mL. The LOD for HL-60 cells was calculated to be 350 cells/mL. Additionally, in situ anticancer drug screening was successfully implemented in this μ-PECD through monitoring of the apoptotic cancer cells by using the fast-response differential pulse voltammetry (DPV) method, after the in-electrode 3D cell culture with anticancer drug-containing culture media. Su et al. [101] further applied the μ-PECD to in-situ evaluation of multi-glycan expressions from living cancer cells. Similarly, Au/paper electrodes were employed and sandwiched with HRP-lectin electrochemical probes for cell detection. Human erythroleukemic cells (K562 cells) were detected with a linear range from 550 to 2.0×10^7 cells/mL with the calculated LOD of 400 cells/mL. The μ-ELPCD was then successfully applied to determine cell-surface multi-glycans expressions on living cells in response to drug treatment through in-electrode 3D cell culture.

Li et al. [102] investigated the influence of paper structures (softwood and hardwood fibers) on the performance of paper-based microfluidic analytical devices in the transport of red blood cells (RBCs) for blood typing. Pore structures were characterized by employing mercury porosimetry. It was shown that hardwood fibers with a low basis weight and higher porosity allowed the easy transport of RBCs and showed high clarity assays in blood-typing. Softwood fibers with more complex pore structure, on other hand, made RBCs transport more difficult and low clarity in blood-typing.

The Whitesides group pioneered a low-cost paper-based microfluidic platform for 3D cell culture to mimic tissue- and organ-level functions [103,104]. They first patterned hydrophobic barriers on individual layers of chromatographic paper by wax printing. Then multiple layers of paper impregnated with suspensions of cells in extracellular matrix hydrogel were stacked to mimic the 3D oxygen and nutrient-gradient architecture *in vivo*. After 3D culture, this stacked paper-based microfluidic platform could be destacked, providing unique layer-by-layer molecular analysis. Cell cultures in the stacked, paper-supported gels provided a flexible platform for the study of genetic response and cell responses to 3D molecular gradients [103].

Li et al. [105] demonstrated a paper-based POC testing disk for multiplexed whole cell bacteria analysis. Antibody conjugated gold nanoparticles were used as the signaling agent for the lateral flow assay (LFA) of whole cell antigens of *Pseudomonas aeruginosa* and *Staphylococcus aureus*. The color intensity of gold nanoparticles accumulated at the testing region was converted to a quantitative voltage reading proportional to the bacterial concentration. The detection range of bacteria was 500–5000 colony-forming units (cfu)/mL for each of the infectious agents tested. Preechakasedkit et al. [106] developed a one-step paper-based immunochromatographic strip test using gold nanoparticles for the rapid detection of *Salmonella typhi* in human serum. Immunoassay was done by binding antigen and antibody from *S. typhi* on a nitrocellulose membrane. The LOD was found to be 1.14×10^5 cfu/mL, which could be visually detected by the naked eye within 15 min.

2.2.2. Food safety analysis

Pesticide residues and foodborne pathogens, present in food or feed products are causing more public health concerns worldwide and are an important safety issue due to their infectiousness and toxicity for human beings. Therefore, the development of low-cost strategies for rapid POC food safety analysis without the need for sophisticated instrumentation is an urgent need. The inexpensive, portable, disposable and easy-to-use microfluidic paper-based sensors have been developed for portable food safety analysis, as summarized in Table 2.

Acetylcholinesterase (AChE) that inhibits chemicals, most notably organophosphate and carbamate pesticides by interfering with or inhibiting cholinesterase, is a major pesticide residue, which can be poisonous to humans [107]. In the body, when such excessive inhibition leads to low levels of cholinesterase, the nervous system can malfunction, and death may result. Therefore, many researchers developed paper-based biosensors for the trace detection of AChE inhibiting chemicals. For example, Hossain et al. [108] reported a paper-based solid-phase biosensor for the detection of AChE inhibitors including paraoxon and aflatoxin B1. This paper-based solid-phase biosensor utilized piezoelectric inkjet printing of biocompatible, enzyme-doped, sol-gel-based inks to create colorimetric sensor strips. Polyvinylamine that captured anionic agents was first printed and then AChE was overprinted by sandwiching the enzyme between two layers of biocompatible sol-gel-derived silica on paper. By measuring the residual activity of AChE on paper, AChE inhibitors were successfully detected using Ellman's colorimetric assay with good LODs, which were ~100 nM for paraoxon and ~30 nM for aflatoxin B1, respectively. This group also developed a reagentless bioactive paper-based solid-phase biosensor for the detection of AChE inhibitors, such as organophosphate pesticides [18]. Good LODs were achieved (bendiocarb ~1 nM; carbaryl ~10 nM; paraoxon ~1 nM; malathion ~10 nM). This bioactive paper-based assay was applied to study pesticide residues collected from food samples such as spiked milk and apple juice. It showed negligible matrix effects and good agreement with a conventional mass spectrometric assay method, demonstrating its applicability for rapid testing of trace levels of organophosphate and carbamate pesticides in food sample analysis. Kavruk et al. [109] developed a paper-based AChE inhibitor sensor for the detection of the degradation products of organophosphorus pesticides. The LOD of malathion was as low as 2.5 ppm. Additionally, among BSA, glucose and trehalose, glucose was found as the best stabilizer in improving color development and shelf-life, especially for visual tests, with the confirmed operational stability by testing 60 days storage at 4 °C. All of these bioassays mentioned above showed good LOD within 5 min. Moreover, qualitative detection was achieved by the naked eye, avoiding the need for sophisticated and expensive instrumentation.

With high severity, frequency of illness and disproportionally high number of fatalities, *Escherichia coli*, *Salmonella spp.*, and *Listeria monocytogenes* are ranked on the top list of pathogenic strains of foodborne bacterial pathogens. Jokerst et al. [110] developed a paper-based microfluidic device for the screening of *E. coli* O157:H7, *Salmonella Typhimurium*, and *L. monocytogenes* in food samples. A paper-based microspot assay was developed by using wax printing on filter paper. Different enzymes associated with the three targeting pathogens reacted with different

Table 2
Summary of food safety analysis on paper-based & its hybrid microfluidic platforms.

Analyte	LOD	Application	Microfluidic platform	Fabrication method	Reference
Paraoxon	~100 nM	Pesticide detection	Paper	Inkjet printing	[108]
Paraoxon	~1 nM	Pesticide detection	Paper	Inkjet printing	[18]
Aflatoxin B1	~30 nM	Pesticide detection	Paper	Inkjet printing	[108]
Bendiocarb	~1 nM	Pesticide detection	Paper	Inkjet printing	[18]
Carbaryl	~10 nM	Pesticide detection	Paper	Inkjet printing	[18]
Malathion	~10 nM	Pesticide detection	Paper	Inkjet printing	[18]
Malathion	2.5 ppm	Pesticide detection	Paper	–	[109]
E. coli	10 cfu/cm^2	Foodborne pathogen	Paper	Wax printing	[110]
L. monocytogenes	10 cfu/cm^2	Foodborne pathogen	Paper	Wax printing	[110]
S. Typhimurium	10 cfu/cm^2	Foodborne pathogen	Paper	Wax printing	[110]
S. Typhimurium	100 cfu/mL	Foodborne pathogen	Paper	Photolithography	[111]
L. acidophilus	11 cfu/mL	Foodborne pathogen	Paper/PDMS	–	[14]
S. enterica	61 cfu/mL	Foodborne pathogen	Paper/PDMS	–	[14]
S. aureus	800 cfu/mL	Foodborne pathogen	Paper/PDMS	–	[14]
Ethanol	0.1 mM	Food quality control	Paper	Wax printing	[112]

chromogenic substrates, leading to different color changes for multiplexed detection. As shown in Fig. 3a, when combined with enrichment procedures (12 h or less), the device was capable of detecting bacteria in concentrations in inoculated ready-to-eat (RTE) meat as low as 10 cfu/cm^2. Park et al. [111] developed a microfluidic paper-based device for quantitative detection of *Salmonella* using a smartphone application. They first preloaded anti-*S. Typhimurium* conjugated submicroparticles in each microfluidic channel of the paper device, then dipped the microfluidic paper device into *Salmonella* solutions, leading to the antibody-conjugated particles confined within the paper fibers to immunoagglutinate. After that, digital images were taken by a smartphone programmed at an optimized angle and distance, from which the extent of immunoagglutination was quantified by evaluating Mie scattering to calculate and display the bacterial concentration. The single-cell-level LOD (from a 10 μL sample) was achieved within one minute, as shown in Fig. 3b.

Monitoring of product shelf life is critical for food quality control and monitoring the incidence of foodborne pathogens. Nie et al. [112] developed a paper-based electrochemical microfluidic device that used a commercial glucometer to measure the concentration of ethanol in food products on site. The calibration plot for the analysis of ethanol showed a linear range from 0.1 to 3 mM, with LOD of 0.1 mM.

3. Paper hybrid microfluidic platforms

Since the advent of microfluidic lab-on-a-chip in the 1990 s, silicon, glass, various polymers, and paper have been used for microfluidic device fabrication. Each material has its own advantages and limitations as well. For example, the ease and low-cost of soft lithography and attractive optical properties of PDMS, have made PDMS microfluidic devices widely used in microfluidic bio-applications [30,113]. However, PDMS microdevices are often associated with additional complicated chemical surface modifications for probe immobilization. Recently, paper-based microfluidic devices have provided a new low-cost platform for different applications related to health care and food safety analysis in low-resource settings [34,38,114,115]. Hydrophobic barriers can be easily patterned

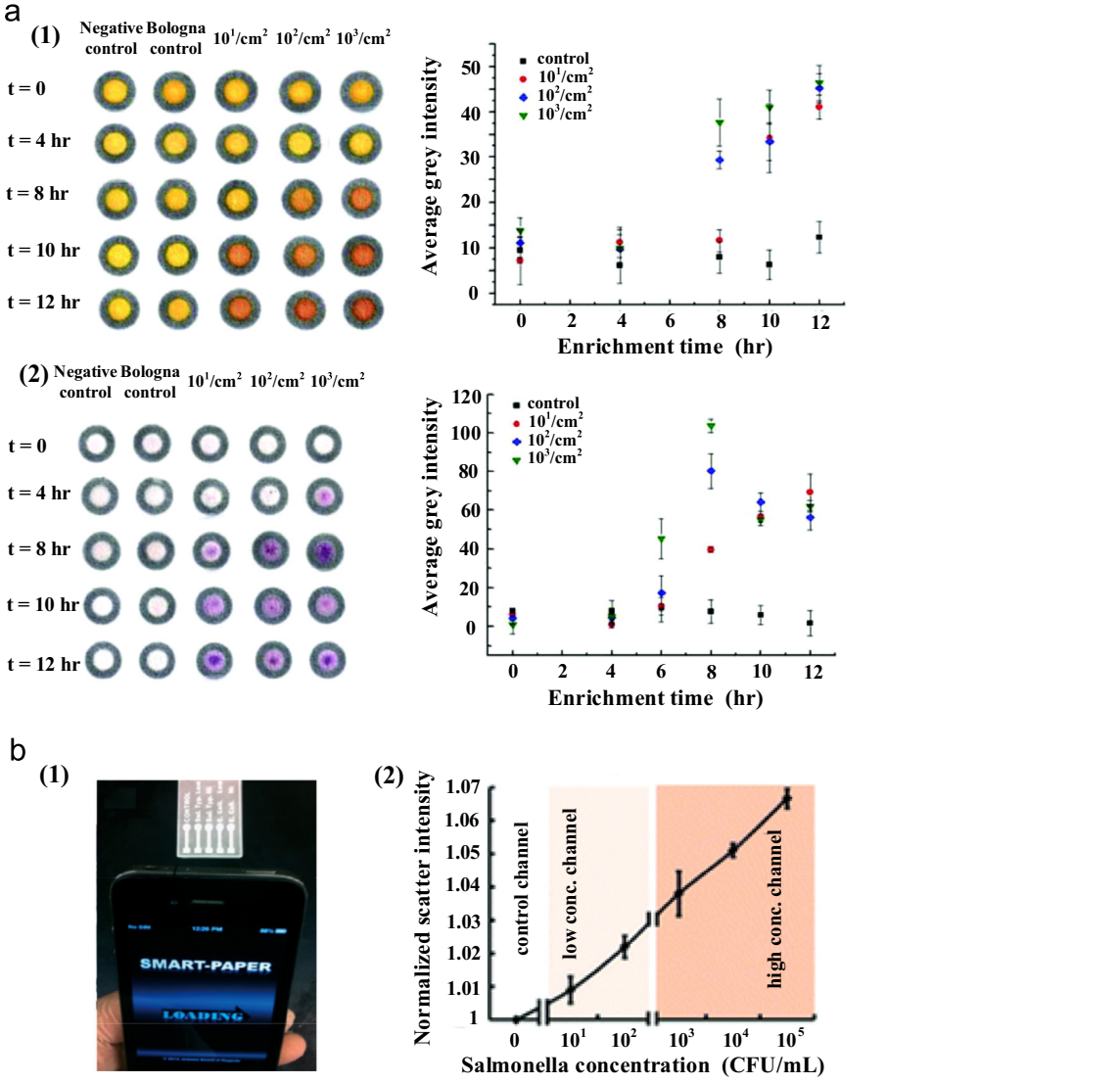

Fig. 3. Microfluidic paper-based devices for the detection of foodborne pathogens. (a) Analysis of ready-to-eat meat samples spiked with 10^1, 10^2, and 10^3 cfu/cm^2 for (1) *E. coli* O157:H7 and (2) *S. Typhimurium*. Enzyme activity of the samples was tested after enrichment of 0, 4, 8, 10, and 12 h. (*Source*: Adapted with permission from Jokerst et al., 2012. Copyright © 2012 American Chemical Society. [110]) (b) Smartphone quantifies *Salmonella* from a paper-based microfluidic paper device. (1) A photograph of the paper-based device with a smartphone launching the smartphone application. (2) A standard calibration curve from the readout of three separate channels using the smartphone application under ambient light (*Source*: Adapted with permission from Park et al., 2013. Copyright © 2013 Royal Society of Chemistry [111]).

on individual layers of chromatographic paper to form microfluidic channels [35], without the stringent requirements of cleanroom facilities. The porous paper is compatible with biological samples, providing a 3D substrate for reagent storage, protection and reaction. Paper-based microfluidic devices, however, typically do not offer the high level of performance and functionality that PDMS affords in liquid flow control and delivery. Therefore, researchers introduced a new type of paper hybrid microfluidic devices (see Tables 1 and 2) that draw benefits from both device substrates [14,15,43,44].

As described earlier, because PDMS microfluidic devices often involved complicated surface modification and paper-based microfluidic devices did not provide high performance in flow control and delivery, the Li group developed the first paper/PDMS hybrid biochip for pathogen detection [14], with aptamer-functionalized graphene oxide (GO) nano-biosensors integrated on the chip for simple, one-step, multiplexed pathogen detection. The porous paper inside detection wells provides a simple 3D substrate for nanosensor immobilization. As shown in Fig. 4, the paper substrate used in this hybrid biochip facilitated the physical absorption of aptamer biosensors, without any complicated surface treatment or aptamer probe immobilization. *Lactobacillus acidophilus* was used as a bacterium model to develop the microfluidic platform with the LOD of 11.0 cfu/mL. This hybrid system has also been successfully extended to the simultaneous detection of two infectious foodborne pathogens (i.e., *Staphylococcus aureus* and *Salmonella enterica*). The one-step 'turn on' pathogen assay in the hybrid microfluidic biochip only took ~10 min to complete.

Although the aforementioned method can directly measure microorganisms without complicated sample preparation due to the use of aptamers, the sensitivity might not be as high as DNA amplification based methods. In order to achieve high detection sensitivity, the Li group developed another paper/PDMS hybrid microfluidic chip integrated with loop-mediated isothermal amplification (LAMP), an isothermal DNA amplification method, for high-sensitivity detection of global infectious diseases [15]. As shown in Fig. 5a and b, chromatography paper disks were placed in LAMP zones, serving as the 3D substrate for DNA primer prestorage for the subsequent LAMP reaction to improve detection sensitivity. It was interesting that they observed that the paper hybrid system enabled much more stable test results over a long period of 2 months than a paper-free microfluidic system (Fig. 5c). Using a centrifuge-free DNA extraction method, they demonstrated high detection sensitivity in the instrument-free detection of the main meningitis-causing bacteria, *Neisseria meningitidis* (*N. meningitidis*). Without use of any specialized instruments, clinical diagnosis of *N. meningitidis* could be achieved by visual confirmation of bright fluorescence with a portable UV light pen, as shown in Fig. 5d. The LOD as low as 3 target DNA copies per LAMP zone was achieved, whereas the current LOD of qPCR is 9 copies per reaction [11]. Recently, a FTA card equipped microcapillary microfluidic system integrated with LAMP has been reported [45], allowing for sample-to-answer screening of single nucleotide polymorphisms (SNPs) typing of the CYP2C19 gene from untreated blood samples. Inside the capillary, all reagents including washing buffer and LAMP mix were preloaded. And the FTA card used to extract DNA from blood samples was inserted into the microcapillary before fluidic operations. Without the requirement for advanced instruments, this microfluidic system can achieve on-site pretreatment, extraction, amplification, and detection of nucleic acids within 150 min. By changing aptamers and primers, these genetic assays using hybrid microfluidic devices have great potential in rapid detection of a wide variety of other infectious pathogens, which is of great significance since the emergence of infectious pathogens has generated extremely significant impact on global health and economies.

Besides nucleic acids analysis, low-cost paper hybrid microfluidic platforms for 3D cell culture have been reported. Qi et al. [116] developed a hydroxypropyl cellulose (HPC) methacrylate composite as a photo-patternable and biodegradable paper hybrid substrate for cell culture and other bio-applications. This hybrid substrate enabled cell proliferation and cell migration in optimal conditions for long-term cell culture and implantable tissue scaffold applications. Deiss et al. [117] reported a paper/PDMS hybrid microfluidic device for culture of bacteria and detection of their resistance to antibiotics using a portable version of the Kirby-Bauer antibiotic susceptibility test (AST). The hybrid device comprised a PDMS membrane and sheets of paper patterned with hydrophobic printer ink and assembled with packing tape. By measuring blue-colored zones of inhibited growth, the antibiotic susceptibility of several strains of *E. coli* and *S. Typhimurium* was quantified. The flexibility of the paper hybrid microfluidic bacterial culture platform should be able to facilitate the integration with

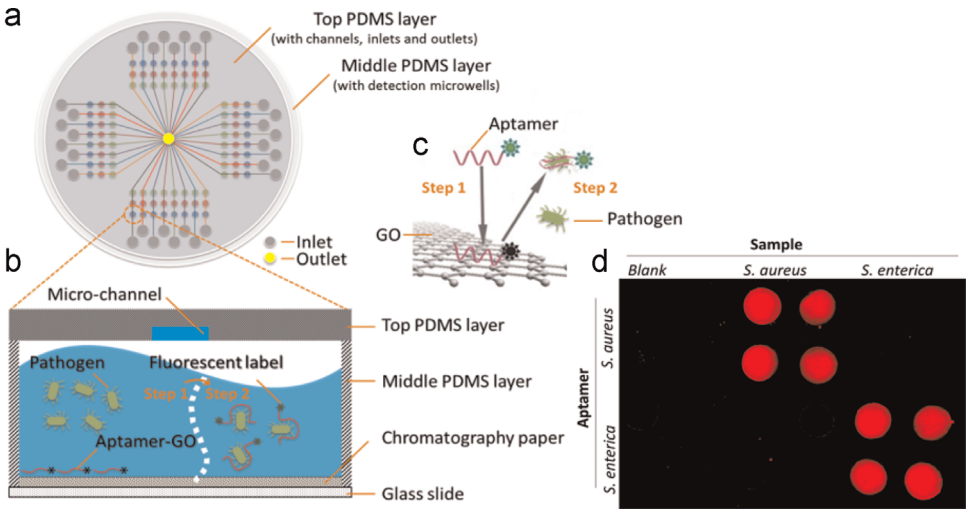

Fig. 4. Schematic of the paper/PDMS hybrid microfluidic biochip for one-step multiplexed pathogen detection using aptamer-functionalized GO biosensors. (a) Microfluidic biochip layout. (b, c) Illustration of the principle of the one-step 'turn-on' detection approach based on the interaction among GO, aptamers and pathogens. When the target pathogen is present, the target pathogen induces the aptamer to be liberated from GO and thereby restores the fluorescence of the aptamer quenched previously by GO. (d) Cross reaction investigation of *Staphylococcus aureus* and *Salmonella enterica* with their corresponding and non-corresponding aptamers (*Source*: Adapted with permission from Zuo et al., 2013. Copyright © 2013 Royal Society of Chemistry [14]).

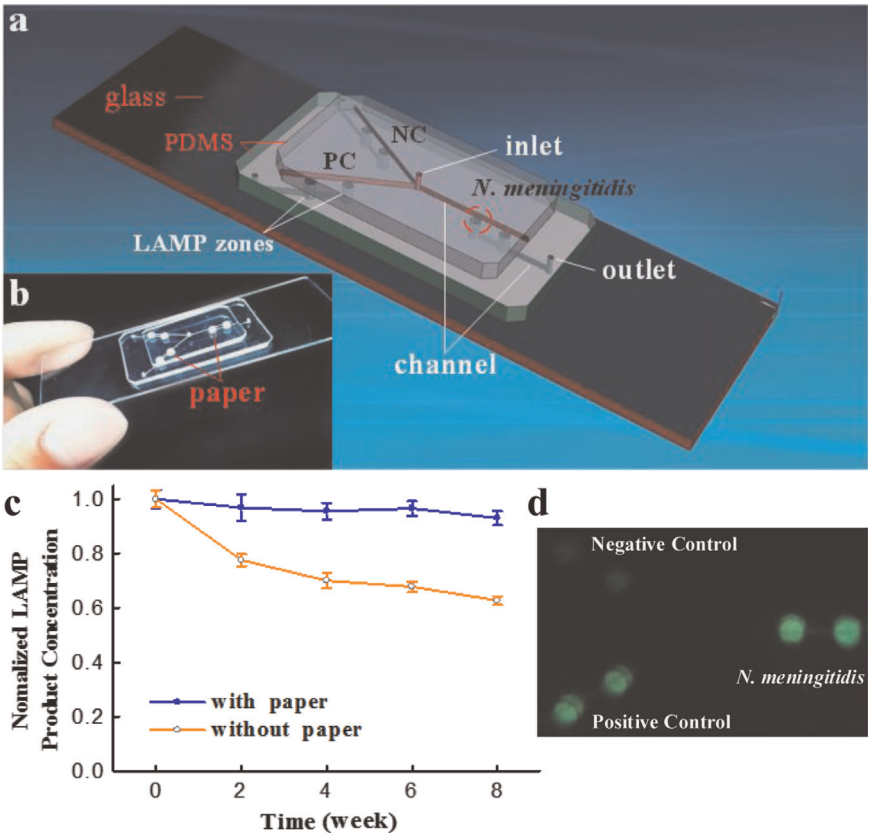

Fig. 5. The paper/PDMS hybrid microfluidic chip integrated with LAMP for high-sensitivity instrument-free infectious disease diagnosis. (a) 3D illustration of the schematic of the chip layout. A chromatography paper disk is situated inside each LAMP zone to preload LAMP primers. (b) A photograph of the hybrid microfluidic chip. (c) On-chip LAMP performance comparison between hybrid microfluidic chip with paper inside and non-hybrid microfluidic chip without paper inside. (d) A fluorescent image taken by a cell phone camera for the on-chip LAMP detection of *N. meningitidis* using a portable UV light pen (*Source*: Adapted with permission from Dou et al., 2014. Copyright © 2014 American Chemical Society [15]).

other paper-based tests, avoiding the need to rely on an external pre-culture of bacteria.

Cotton thread is another low-cost platform with good wicking property and flexibility. Its one-dimensional (1D) characteristics made it unnecessary to create new hydrophobic barriers when transferring liquids, but it is challenging to carry out quantitative analysis. Thus, 1D cotton threads and 2D paper sheets have been combined to form another type of paper hybrid microfluidic platforms [43,44]. The combination of 1D materials with other 2D materials makes it feasible to fabricate 3D microfluidic devices. The fabrication of the paper/thread 3D microfluidic platforms requires only commonly used and affordable sewing needles or household sewing machines. In such a hybrid microfluidic platform, a thread acts as a 3D passageway in sewn materials, which can transport liquid via capillary wicking without the need of a barrier. This paper/thread hybrid microfluidic platform can be used for qualitative or semiquantitative analysis. Li et al. [43] demonstrated thread/paper-based sensors with the incorporated colorimetric indicators for detection of nitrite ion (NO_2^-) and uric acid (UA), which are two important biomarkers of several human medical conditions. A test solution was introduced onto the threads from the central film hole with a micropipette; the test solution rapidly wicked along the threads and reached paper disks pre-treated with NO_2^- or the UA indicators, leading to color changes for colorimetric detection. Lin et al. [44] developed another paper/cotton hybrid microfluidic device for in vitro diagnostics. The device used cotton as a flow channel and chromatography paper as reaction zones to obtain semi-quantitative information. The color intensity was distinguishable by the naked eye and can be further analyzed by the software ImageJ for semi-quantitative analysis. By using artificial samples, clinically relevant ranges of approximately 0.38–30 mM for urine protein, 0.16–2.5 mM for NO_2^-, 7.80–125 mM for urobilinogen and 100–1600 mM for UA were analyzed.

4. Conclusions and perspectives

Because of its low cost and ease of fabrication, enormous paper-based microfluidic devices have been developed for various applications in disease diagnosis, food safety inspection and even environmental analysis, especially for resource-poor settings, such as rural areas and developing nations where people cannot afford costly instrumentation. Various bio-applications of paper-based microfluidic devices have been demonstrated through immunoassay, nucleic acid analysis and cellular analysis (see Tables 1 and 2).

Despite many advantages of paper, the material is not 'perfect'. As mentioned in the Paper Hybrid Microfluidic Platforms Section, each device substrate has its own advantages and limitations. Since the advent of the concept of paper hybrid microfluidic devices from the Li group [14,15], many new paper hybrid systems have been developed. Researchers have demonstrated new benefits that used to be impossible in non-hybrid systems, from paper hybrid microfluidic platforms. We believe that more and more paper hybrid devices will be developed and that they will play an increasingly important role in the near future. However, some technological challenges might need to be addressed to create seamless and high-resolution hybrid devices from two different device substrates, because current fabrication methods for paper-

based devices do not offer high resolution. Some fabrication methods (e.g. through high temperature) might damage original paper properties.

Paper-based devices are inexpensive. However, certain detectors are still bulky and costly, which limits the applications of paper-based devices in low-resource settings. Multiple detection strategies have been used in paper-based microfluidic analysis such as colorimetric, fluorescence, chemiluminescence, ECL and electrochemical detection. Colorimetric detection is highly compatible with the nature of low-cost assay in low-resource settings, but the sensitivity and quantitation are often compromised. Electrochemical detection is also desirable for paper-based microfluidic devices, but the bulky and expensive potentiostat is a bottleneck. Although portable potentiostats are commercially available, the cost is still fairly high. Chemiluminescence does not require complicated optical setup; therefore it is also a preferred detection method for paper-based devices in low-resource settings. In the last decades, smartphone technologies have developed dramatically. Powerful CPU chips have been used in smartphones. An increasing number of new applications and add-ons enabled those smartphones to offer more and more functions for monitoring personal health status [10,15]. Therefore, we envision that the combination of smartphone technologies or other inexpensive electronic readers (e.g. glucometers [112]) with paper-based microfluidic devices could cause great impacts on health care and environmental monitoring in the near future.

Acknowledgment

The Li group would like to acknowledge the financial support of the National Institute of Allergy and Infectious Diseases of the National Institutes of Health (NIH) under Award Number R21AI107415, and the National Institute of General Medical Sciences of the NIH under Award Number SC2GM105584. The content is solely the responsibility of the authors and does not necessarily represent the official views of the NIH. Financial supports from the IDR Program at the University of Texas at El Paso (UTEP) and the NIH RCMI Pilot Grant are also gratefully acknowledged. F.X. would like to acknowledge the financial support of the Key (Key grant) Project of Chinese Ministry of Education (313045) and International Science & Technology Cooperation Program of China (2013DFG02930).

References

[1] X.J. Li, Y. Zhou, Microfluidic Devices for Biomedical Applications, Woodhead Publishing, Philadelphia, USA, 2013.
[2] C.T. Culbertson, T.G. Mickleburgh, S.A. Stewart-James, K.A. Sellens, M. Pressnall, Anal. Chem. 86 (2013) 95–118.
[3] X.J. Li, A.V. Valadez, P. Zuo, Z. Nie, Bioanalysis 4 (2012) 1509–1525.
[4] X. Li, P.C.H. Li, Expert Rev. Clin. Pharmacol. 3 (2010) 267–280.
[5] G.B. Salieb-Beugelaar, G. Simone, A. Arora, A. Philippi, A. Manz, Anal. Chem. 82 (2010) 4848–4864.
[6] M.L. Kovarik, P.C. Gach, D.M. Ornoff, Y. Wang, J. Balowski, L. Farrag, N.L. Allbritton, Anal. Chem. 84 (2011) 516–540.
[7] F. Yang, X. Zuo, Z. Li, W. Deng, J. Shi, G. Zhang, Q. Huang, S. Song, C. Fan, Adv. Mater. 26 (2014) 4671–4676.
[8] X. Fang, S. Wei, J. Kong, Lab Chip 14 (2014) 911–915.
[9] X.J. Li, P.C.H. Li, Can. J. Pure Appl. Sci., 8, (2014) 2663–2669.
[10] X. Xu, A. Akay, H. Wei, S. Wang, B. Pingguan-Murphy, B. Erlandsson, X. Li, W. Lee, J. Hu, L. Wang, F. Xu, Proc. IEEE 103 (2015) 236–247.
[11] X. Wang, M.J. Theodore, R. Mair, E. Trujillo-Lopez, M. du Plessis, N. Wolter, A.L. Baughman, C. Hatcher, J. Vuong, L. Lott, J. Clin. Microbiol. 50 (2012) 702–708.
[12] F. Perini, A. Casabianca, C. Battocchi, S. Accoroni, C. Totti, A. Penna, PLoS One 6 (2011) e17699.
[13] L. Ge, J. Yan, X. Song, M. Yan, S. Ge, J. Yu, Biomaterials 33 (2012) 1024–1031.
[14] P. Zuo, X. Li, D.C. Dominguez, B.-C. Ye, Lab Chip 13 (2013) 3921–3928.
[15] M. Dou, D.C. Dominguez, X. Li, J. Sanchez, G. Scott, Anal. Chem. 86 (2014) 7978–7986.
[16] S. Wang, F. Xu, U. Demirci, Biotechnol. Adv. 28 (2010) 770–781.
[17] M.E.I. Badawy, A.F. El-Aswad, Int. J. Anal. Chem. 2014 (2014) 8.
[18] S.Z. Hossain, R.E. Luckham, M.J. McFadden, J.D. Brennan, Anal. Chem. 81 (2009) 9055–9064.
[19] Z. Nie, C.A. Nijhuis, J. Gong, X. Chen, A. Kumachev, A.W. Martinez, M. Narovlyansky, G.M. Whitesides, Lab Chip 10 (2010) 477–483.
[20] A. Apilux, W. Dungchai, W. Siangproh, N. Praphairaksit, C.S. Henry, O. Chailapakul, Anal. Chem. 82 (2010) 1727–1732.
[21] A.W. Martinez, S.T. Phillips, G.M. Whitesides, Proc. Natl. Acad. Sci. USA 105 (2008) 19606–19611.
[22] A.J. Chung, D. Kim, D. Erickson, Lab Chip 8 (2008) 330–338.
[23] X.J. Li, Y.C. Chen, P.C.H. Li, Lab Chip 11 (2011) 1378–1384.
[24] X.J. Li, X. Xue, P.C.H. Li, Integr. Biol. 1 (2009) 90–98.
[25] X.J. Li, V. Ling, P.C.H. Li, Anal. Chem. 80 (2008) 4095–4102.
[26] X.J. Li, J. Huang, G.F. Tibbits, P.C.H. Li, Electrophoresis 28 (2007) 4723–4733.
[27] X.J. Li, P.C.H. Li, Anal. Chem. 77 (2005) 4315–4322.
[28] F. Shen, X. Li, P.C.H. Li, Biomicrofluidics 8 (2014) 014109.
[29] H. Chen, X. Li, L. Wang, P.C. Li, Talanta 81 (2010) 1203–1208.
[30] Y. Xia, G.M. Whitesides, Annu. Rev. Mater. Sci. 1998 (1998) 153–184.
[31] X. Fang, Y. Liu, J. Kong, X. Jiang, Anal. Chem. 82 (2010) 3002–3006.
[32] W. Liu, C.L. Cassano, X. Xu, Z.H. Fan, Anal. Chem. 85 (2013) 10270–10276.
[33] X. Li, Z. Nie, C. Cheng, A. Goodale, G. Whitesides, Proc. Micro Total Anal. Syst. (2010) 1487–1489.
[34] Z. Nie, C.A. Nijhuis, J. Gong, X. Chen, A. Kumachev, A.W. Martinez, M. Narovlyansky, G.M. Whitesides, Lab Chip 10 (2010) 477–483.
[35] C.M. Cheng, A.W. Martinez, J. Gong, C.R. Mace, S.T. Phillips, E. Carrilho, K.A. Mirica, G.M. Whitesides, Angew. Chem. Int. Ed. Engl. 49 (2010) 4771–4774.
[36] Y.L. Han, W. Wang, J. Hu, G. Huang, S. Wang, W.G. Lee, T.J. Lu, F. Xu, Lab Chip 13 (2013) 4745–4749.
[37] A.W. Martinez, S.T. Phillips, M.J. Butte, G.M. Whitesides, Angew. Chem. Int. Ed. 46 (2007) 1318–1320.
[38] X.Y. Liu, M. Mwangi, X.J. Li, M. O'Brien, G.M. Whitesides, Lab Chip 11 (2011) 2189–2196.
[39] J. Hu, S. Wang, L. Wang, F. Li, B. Pingguan-Murphy, T.J. Lu, F. Xu, Biosens. Bioelectron. 54 (2014) 585–597.
[40] K. Abe, K. Kotera, K. Suzuki, D. Citterio, Anal. Bioanal. Chem. 398 (2010) 885–893.
[41] M. Nogi, S. Iwamoto, A.N. Nakagaito, H. Yano, Adv. Mater. 21 (2009) 1595–1598.
[42] H. Zhu, Z. Fang, C. Preston, Y. Li, L. Hu, Energy Environ. Sci. 7 (2014) 269–287.
[43] X. Li, J. Tian, W. Shen, ACS Appl. Mater. Interfaces 2 (2009) 1–6.
[44] S.-C. Lin, M.-Y. Hsu, C.-M. Kuan, H.-K. Wang, C.-L. Chang, F.-G. Tseng, C.-M. Cheng, Sci. Reports 4 (2014).
[45] L. Zhang, Y. Zhang, C. Wang, Q. Feng, F. Fan, G. Zhang, X. Kang, X. Qin, J. Sun, Y. Li, Anal. Chem. 86 (2014) 10461–10466.
[46] A.W. Martinez, S.T. Phillips, G.M. Whitesides, E. Carrilho, Anal. Chem. 82 (2009) 3–10.
[47] E.M. Fenton, M.R. Mascarenas, G.P. López, S.S. Sibbett, ACS Appl. Mater. Interfaces 1 (2008) 124–129.
[48] X. Li, J. Tian, G. Garnier, W. Shen, Coll. Surf. B, Biointerfaces 76 (2010) 564–570.
[49] J. Yu, L. Ge, J. Huang, S. Wang, S. Ge, Lab Chip 11 (2011) 1286–1291.
[50] A.W. Martinez, S.T. Phillips, E. Carrilho, S.W. Thomas 3rd, H. Sindi, G.M. Whitesides, Anal. Chem. 80 (2008) 3699–3707.
[51] R.F. Carvalhal, M.S. Kfouri, M.H. Piazetta, A.L. Gobbi, L.T. Kubota, Anal. Chem. 82 (2010) 1162–1165.
[52] A.K. Ellerbee, S.T. Phillips, A.C. Siegel, K.A. Mirica, A.W. Martinez, P. Striehl, N. Jain, M. Prentiss, G.M. Whitesides, Anal. Chem. 81 (2009) 8447–8452.
[53] A.W. Martinez, S.T. Phillips, Z. Nie, C.M. Cheng, E. Carrilho, B.J. Wiley, G.M. Whitesides, Lab Chip 10 (2010) 2499–2504.
[54] T. Songjaroen, W. Dungchai, O. Chailapakul, W. Laiwattanapaisal, Talanta 85 (2011) 2587–2593.
[55] S.M.Z. Hossain, R.E. Luckham, A.M. Smith, J.M. Lebert, L.M. Davies, R.H. Pelton, C.D.M. Filipe, J.D. Brennan, Anal. Chem. 81 (2009) 5474–5483.
[56] P. Wang, L. Ge, M. Yan, X. Song, S. Ge, J. Yu, Biosens. Bioelectron. 32 (2012) 238–243.
[57] A. Arena, N. Donato, G. Saitta, A. Bonavita, G. Rizzo, G. Neri, Sens. Actuators B: Chem. 145 (2010) 488–494.
[58] M. Cretich, V. Sedini, F. Damin, M. Pelliccia, L. Sola, M. Chiari, Anal. Biochem. 397 (2010) 84–88.
[59] R. Hawkes, E. Niday, J. Gordon, Anal. Biochem. 119 (1982) 142–147.
[60] C.M. Cheng, A.W. Martinez, J. Gong, C.R. Mace, S.T. Phillips, E. Carrilho, K.A. Mirica, G.M. Whitesides, Angew. Chem. Int. Ed. 49 (2010) 4771–4774.
[61] Y. Lu, W. Shi, J. Qin, B. Lin, Anal. Chem. 82 (2009) 329–335.
[62] Y. Lu, W. Shi, L. Jiang, J. Qin, B. Lin, Electrophoresis 30 (2009) 1497–1500.
[63] A. Li, Y. Wang, L. Deng, X. Zhao, Q. Yan, Y. Cai, J. Lin, Y. Bai, S. Liu, Y. Zhang, Cytotechnology (2012) 1–11.
[64] D.A. Bruzewicz, M. Reches, G.M. Whitesides, Anal. Chem. 80 (2008) 3387–3392.
[65] K. Abe, K. Suzuki, D. Citterio, Anal. Chem. 80 (2008) 6928–6934.
[66] E. Carrilho, A.W. Martinez, G.M. Whitesides, Anal. Chem. 81 (2009) 7091–7095.
[67] W. Dungchai, O. Chailapakul, C.S. Henry, The Analyst 136 (2011) 77–82.

[68] J. Olkkonen, K. Lehtinen, T. Erho, Anal. Chem. 82 (2010) 10246–10250.
[69] X. Li, J. Tian, T. Nguyen, W. Shen, Anal. Chem. 80 (2008) 9131–9134.
[70] X. Li, J. Tian, W. Shen, Cellulose 17 (2010) 649–659.
[71] X. Li, J. Tian, W. Shen, Anal. Bioanal. Chem. 396 (2010) 495–501.
[72] V. Gauvreau, G. Laroche, Bioconjug. Chem. 16 (2005) 1088–1097.
[73] R.M. Nagler, Clin. Chem. 54 (2008) 1415–1417.
[74] G. Chitnis, Z. Ding, C.L. Chang, C.A. Savran, B. Ziaie, Lab Chip 11 (2011) 1161–1165.
[75] A.W. Martinez, S.T. Phillips, G.M. Whitesides, Proc. Natl. Acad. Sci. USA 105 (2008) 19606–19611.
[76] X.J. Li, W.R. Jin, Q.F. Weng, Anal. Chim. Acta 461 (2002) 123–130.
[77] W.R. Jin, X.J. Li, N. Gao, Anal. Chem. 75 (2003) 3859–3864.
[78] X.J. Li, W.R. Jin, Chin. Chem. Lett. 13 (2002) 874–876.
[79] I.M. Thompson, D.K. Pauler, P.J. Goodman, C.M. Tangen, M.S. Lucia, H. L. Parnes, L.M. Minasian, L.G. Ford, S.M. Lippman, E.D. Crawford, N. Engl. J. Med. 350 (2004) 2239–2246.
[80] E. Engvall, P. Perlmann, Immunochemistry 8 (1971) 871–874.
[81] S. Kivity, B. Gilburd, N. Agmon-Levin, M.G. Carrasco, Y. Tzafrir, Y. Sofer, M. Mandel, T. Buttner, D. Roggenbuck, M. Matucci-Cerinic, Clin. Rheumat. 31 (2012) 503–509.
[82] N. Latif, C.S. Baker, M.J. Dunn, M.L. Rose, P. Brady, M.H. Yacoub, J. Am. Coll. Cardiol. 22 (1993) 1378–1384.
[83] J. Brouwer, Int. Arch. Allergy Immunol. 85 (1988) 244–249.
[84] A. Singh, S. Datta, A. Sachdeva, S. Maslanka, J. Dykes, G. Skinner, D. Burr, R.C. Whiting, S.K. Sharma, Health Secur. (2015).
[85] J. Kai, A. Puntambekar, N. Santiago, S.H. Lee, D.W. Sehy, V. Moore, J. Han, C.H. Ahn, Lab Chip 12 (2012) 4257–4262.
[86] T. Songjaroen, W. Dungchai, O. Chailapakul, C.S. Henry, W. Laiwattanapaisal, Lab Chip 12 (2012) 3392–3398.
[87] S. Wang, L. Ge, X. Song, J. Yu, S. Ge, J. Huang, F. Zeng, Biosens. Bioelectron. 31 (2012) 212–218.
[88] W. Li, M. Li, S. Ge, M. Yan, J. Huang, J. Yu, Anal. Chim. Acta 767 (2013) 66–74.
[89] J. Liang, Y. Wang, B. Liu, RSC Adv. 2 (2012) 3878–3884.
[90] A. Yu, J. Shang, F. Cheng, B.A. Paik, J.M. Kaplan, R.B. Andrade, D.M. Ratner, Langmuir 28 (2012) 11265–11273.
[91] Y. Chen, H. Cheng, K. Tram, S. Zhang, Y. Zhao, L. Han, Z. Chen, S. Huan, Analyst 138 (2013) 2624–2631.
[92] P. Liu, X. Li, S.A. Greenspoon, J.R. Scherer, R.A. Mathies, Lab Chip 11 (2011) 1041–1048.
[93] S. Poppert, A. Essig, B. Stoehr, A. Steingruber, B. Wirths, S. Juretschko, U. Reischl, N. Wellinghausen, J. Clin. Microbiol. 43 (2005) 3390–3397.
[94] A.C. Araújo, Y. Song, J. Lundeberg, P.L. Ståhl, H. Brumer, Anal. Chem. 84 (2012) 3311–3317.
[95] S.J. Lo, S.C. Yang, D.J. Yao, J.H. Chen, C.M. Cheng, IEEE Nanotechnol. Mag. 6 (2012) 26–30.
[96] J.C. Cunningham, N.J. Brenes, R.M. Crooks, Anal. Chem. 86 (2014) 6166–6170.
[97] P. Ihalainen, F. Pettersson, M. Pesonen, T. Viitala, A. Määttänen, R. Österbacka, J. Peltonen, Nanotechnology 25 (2014) 094009.
[98] Y. Wang, L. Ge, P. Wang, M. Yan, S. Ge, N. Li, J. Yu, J. Huang, Lab Chip 13 (2013) 3945–3955.
[99] L. Wu, C. Ma, L. Ge, Q. Kong, M. Yan, S. Ge, J. Yu, Biosens. Bioelectron. 63 (2015) 450–457.
[100] M. Su, L. Ge, S. Ge, N. Li, J. Yu, M. Yan, J. Huang, Anal. Chim. Acta 847 (2014) 1–9.
[101] M. Su, L. Ge, Q. Kong, X. Zheng, S. Ge, N. Li, J. Yu, M. Yan, Biosens. Bioelectron. 63 (2015) 232–239.
[102] L. Li, X. Huang, W. Liu, W. Shen, ACS Appl. Mater. Interfaces 6 (2014) 21624–21631.
[103] R. Derda, A. Laromaine, A. Mammoto, S.K. Tang, T. Mammoto, D.E. Ingber, G.M. Whitesides, Proc. Natl. Acad. Sci. USA 106 (2009) 18457–18462.
[104] R. Derda, S.K. Tang, A. Laromaine, B. Mosadegh, E. Hong, M. Mwangi, A. Mammoto, D.E. Ingber, G.M. Whitesides, PLoS One 6 (2011) e18940.
[105] C.-z Li, K. Vandenberg, S. Prabhulkar, X. Zhu, L. Schneper, K. Methee, C.J. Rosser, E. Almeide, Biosens. Bioelectron. 26 (2011) 4342–4348.
[106] P. Preechakasedkit, K. Pinwattana, W. Dungchai, W. Siangproh, W. Chaicumpa, P. Tongtawe, O. Chailapakul, Biosens. Bioelectron. 31 (2012) 562–566.
[107] G. Mercey, T. Verdelet, J. Renou, M. Kliachyna, R. Baati, F. Nachon, L. Jean, P.-Y. Renard, Acc. Chem. Res. 45 (2012) 756–766.
[108] S.M.Z. Hossain, R.E. Luckham, M.J. McFadden, J.D. Brennan, Anal. Chem. 81 (2009) 9055–9064.
[109] M. Kavruk, V.C. Özalp, H.A. Öktem, J. Anal. Methods Chem. 2013 (2013) 8.
[110] J.C. Jokerst, J.A. Adkins, B. Bisha, M.M. Mentele, L.D. Goodridge, C.S. Henry, Anal. Chem. 84 (2012) 2900–2907.
[111] T. San Park, W. Li, K.E. McCracken, J.-Y. Yoon, Lab Chip 13 (2013) 4832–4840.
[112] Z. Nie, F. Deiss, X. Liu, O. Akbulut, G.M. Whitesides, Lab Chip 10 (2010) 3163–3169.
[113] S.K.Y. Tang, G.M. Whitesides, Optofluid.: Fundam., Devices Appl. (2010) 7–31.
[114] X.J. Li, Z.H. Nie, C.-M. Cheng, A.B. Goodale, G.M. Whitesides, Proc. Micro Total Anal. Syst. 14 (2010) 1487–1489.
[115] A.W. Martinez, S.T. Phillips, G.M. Whitesides, E. Carrilho, Anal. Chem. 82 (2010) 3–10.
[116] A. Qi, S.P. Hoo, J. Friend, L. Yeo, Z. Yue, P.P. Chan, Adv. Healthc. Mater. 3 (2014) 543–554.
[117] F. Deiss, M.E. Funes-Huacca, J. Bal, K.F. Tjhung, R. Derda, Lab Chip 14 (2014) 167–171.